Studies on Inducing Cancer Cell Death and Required Light Energy by Photodynamic Therapy Using Wireless Power Transfer

Yoshitaka YASUDA
Faculty of Science and Technology
Tokyo University of Science
Noda, Japan

Takehiro IMURA
Faculty of Science and Technology
Tokyo University of Science
Noda, Japan

Yoichi HORI
Faculty of Science and Technology
Tokyo University of Science
Noda, Japan

Kenta YOKOI
Faculty of Pharmaceutical Sciences
Tokyo University of Science
Noda, Japan

Azusa KANBE
Faculty of Pharmaceutical Science
Tokyo University of Science
Noda, Japan

Masaki KAKIHANA
Faculty of Pharmaceutical Science
Tokyo University of Science
Noda, Japan

Shin AOKI
Faculty of Pharmaceutical Science
Tokyo University of Science
Noda, Japan

***Abstract*—Recently, Photodynamic Therapy(PDT) using light has been expected as a low-invasive treatment because it has fewer side effects than conventional cancer treatment. However, current PDT is limited to the types of cancer that can be reached by cables, so it is difficult to apply PDT to cancers deep inside the body, such as pancreatic cancer. In this paper, we designed a wireless power transfer system that combines a small and lightweight receiving coil and LEDs for implantation in the body. After that, we experimented to see whether cancer cell death was induced by photoirradiation in vitro using power transfer in free air space. As a result, we succeeded in inducing about 75 % of cancer cell death by 60 minutes of photoirradiation at a 30 mm transfer distance. At that time, we derived an approximation of the amount of light energy required to induce cancer cell death by changing the photoirradiation time, and we were able to predict the treatment time.**

Keywords—Wireless Power Transfer, Magnetic Resonant Coupling, 6.78 MHz, Photodynamic Therapy, Cancer Treatment

I. INTRODUCTION

Recently, wireless power transfer (WPT), which transfers power to various devices without cables, has been studied widely [1]. By the establishment of technology using resonance, it enables higher efficiency and power transfer with a large air gap than conventional WPT, so it has been investigated for application in a wide range of fields, from electric vehicles [2-4] to smartphones [5, 6]. Among them, WPT for implantable devices such as the ventricular assist device [7, 8] and the cochlear implant [9] has attracted much attention as a method to enhance the QOL of patients due to its low invasiveness [10-12]. This technology eliminates the risk of surgery to replace batteries used in implantable devices in the body, infections caused by cables penetrating the skin, and battery breakage in the body because it becomes unnecessary to replace batteries or to supply power via cables from an external power source.

In this paper, we focus on the application to the medical field and target the integration of WPT and photodynamic therapy, a type of cancer treatment, at 6.78 MHz allocated in the ISM band. We designed a small and lightweight WPT device that can emit visible light using LEDs and evaluated it mainly in terms of radiant flux. After that, we verified the significance through the induction of cancer cell death in vitro. Moreover, we derive an approximation of the amount of light energy required based on the percentage of induced cell death for each photoirradiation time in cell experiments, and indicate that it is possible to predict the treatment time using this system.

Chapter 2 describes the mechanism of action of photodynamic therapy and its relation to WPT, and Chapter 3 describes the design of the WPT system. In Chapter 4, the designed system is evaluated in terms of engineering and pharmaceutics, and in Chapter 5, we describe cell death induction experiments in vitro using cancer cells. Chapter 6 discusses the amount of light energy required for treatment and the treatment time, and finally, Chapter 7 presents the conclusions.

II. PHOTODYNAMIC THERAPY

A. About Photodynamic Therapy

Various treatments for cancer, the leading cause of death globally and the first of the three leading causes of death in Japan, are being researched internationally. Currently, surgery, chemotherapy, and radiation therapy are the three main established methods of cancer treatment. However, each method of cancer treatment has its own problems, such as physical burden, side effects, metastasis, and recurrence, and various new methods of cancer treatment, such as immunotherapy and targeted therapy, are being researched.

In this paper, we focus on one of these treatments, photodynamic therapy (PDT). PDT is a method of cancer treatment in which a photosensitizer that accumulates specifically on cancer cells is administered, followed by irradiation of cancer cells with light of a specific wavelength. As shown in the PDT mechanism of action in Fig. 1, cancer cell death is induced by generating singlet oxygen, a type of reactive oxygen species (ROS) that poses cytotoxicity within cancer cells. This treatment has less adverse effects on normal tissues and fewer side effects than existing treatments. In addition, it is said to induce damage or occlusion of nutrient blood vessels around cancer, thereby obtaining an anti-tumor effect through a secondary action. In Japan, insurance coverage is applicable to lung cancer, esophageal cancer, gastric cancer, and malignant brain tumors using two types of photosensitizers: first-generation porfimer sodium and second-generation talaporfin sodium. However, current PDT

is limited to applicable cancers, because laser irradiation is mainly performed by a combination of endoscopes and fiber-optic cables. Therefore, it is difficult to apply to cancers deep inside the body, such as pancreatic cancer.

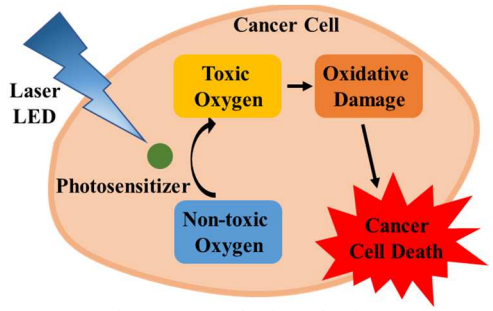

Fig. 1 PDT mechanism of action

B. *Advantages of WPT+PDT*

Although photo-irradiation of cancer with wire described in the previous section is basically completed in a single treatment, multiple photo-irradiations are desirable for more effective treatment [13]. So, implanting a light source for treatment in the body has been proposed, but there are only a few studies integrating WPT and PDT [14-16]. In addition, the transfer distance in those studies was short, and their application to cancers deep inside the body has not been considered. In this paper, we intend to integrate WPT and PDT as shown in Fig. 2, and verify their significance by basic experiments using cancer cells in vitro. By doing so, we can contribute to future cancer treatment through the possibility of minimally invasive approaches to cancers deep inside the body, which are difficult to apply with current methods of cancer treatment. In addition, multidisciplinary treatment combined with other treatment methods including surgery reduces the recurrence risk caused by residual tissue, and the elimination of the need for repeated surgery provides flexible treatment at recurrence. By wirelessly PDT, which was previously performed by wire, there has been expected number of advantages.

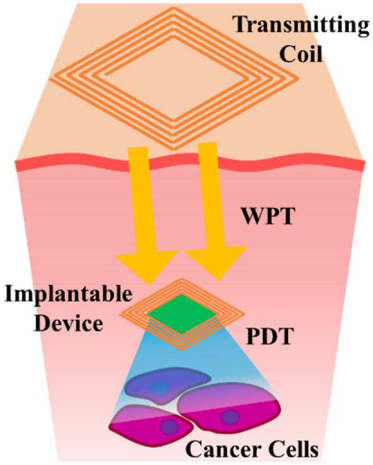

Fig. 2 Image of cancer treatment with WPT+PDT [17]

III. WPT STSTEM DESIGN

Radiation type using microwaves or ultrasonic waves [18, 19] and coupling type using magnetic fields or electric fields [20, 21] are the main methods of WPT, but in this paper, we focus on WPT using magnetic fields. The wireless power transfer circuit to be used is a series(S)-parallel(P) topology magnetic field resonance circuit, in which capacitors and inductors are connected in series on the transmitting side and connected in parallel on the receiving side to resonate. The equivalent circuit diagram is shown in Fig. 3. It is necessary to have internal control circuits to prevent malfunction when supplying power for clinical applications, but in this paper, we have not considered them for the purpose of verifying the significance of the system. In determining the topology, the circuit was simulated with four topologies (S-S, S-P, P-S, and P-P). Variation of the current value of the LEDs, which are the load on the receiving side, was simulated by varying the transfer distance with an input voltage of 10 V. In this paper, the input voltages are RMS values because they are AC voltages. The results are shown in Fig. 4. As shown in Fig. 4, the S-S, P-S, and P-P topologies do not provide enough current to operate the LEDs, so the S-P topology, which provides linear current even at low coupling, is adopted in this paper. The fabricated transmitting and receiving devices are shown in Fig. 5, and their respective specifications are shown in Table 1.

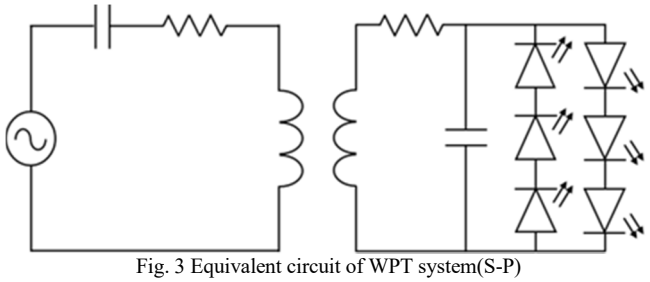

Fig. 3 Equivalent circuit of WPT system(S-P)

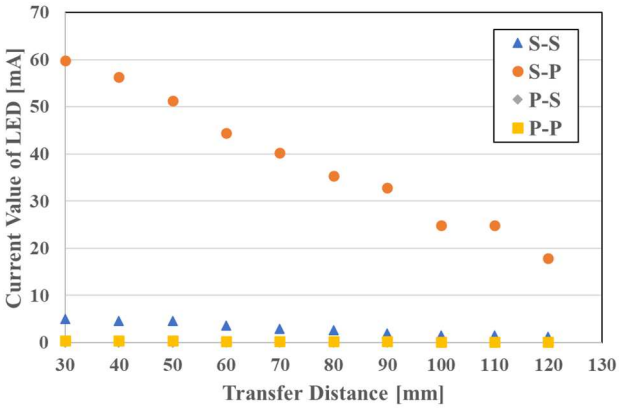

Fig. 4 The result of simulations of the relation between transmitting and receiving devices(30-120 mm) and the current values of the LED on the receiving device in four basic topologies(S-S, S-P, P-S, P-P).

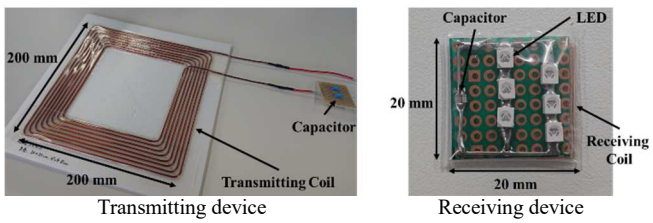

Transmitting device Receiving device

Fig. 5 Pictures of transmitting and receiving devices

Table 1 Specifications of experimental equipment

	Transmitting Side	Receiving Side
Size [mm]	200×200	20×20
Number of turns	8	6
Q value	449	83.0
Resistance [Ω]	2.35	0.55
Inductance [μH]	24.6	1.07
Capacitance [pF]	23.5	508

IV. Evaluation of the WPT System

A. Measurement of Radiant Flux from LEDs

The radiant flux from the LEDs that emit blue light on the receiving device was measured using the experimental equipment shown in Fig. 6. The operating frequency is set to 6.78 MHz, the input voltage is 8-10 V, and the transfer distance is 30-120 mm. When measuring the radiant flux, we considered the 15 mm space that exists between the cell surface to be cultured in the well plate and the emitting surface of the LED. As shown in Fig. 7, the radiant flux from the LEDs on the receiving device was increased as the input voltage increased and decreased as the transfer distance increased.

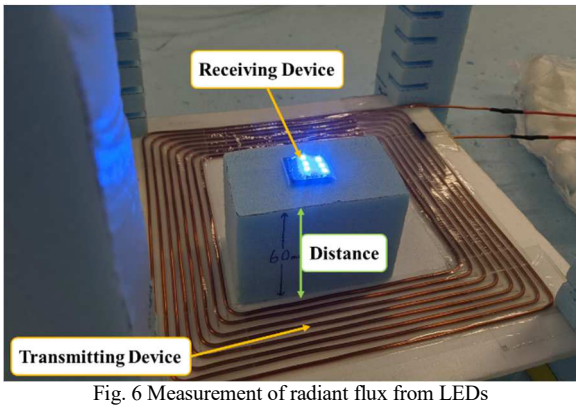

Fig. 6 Measurement of radiant flux from LEDs

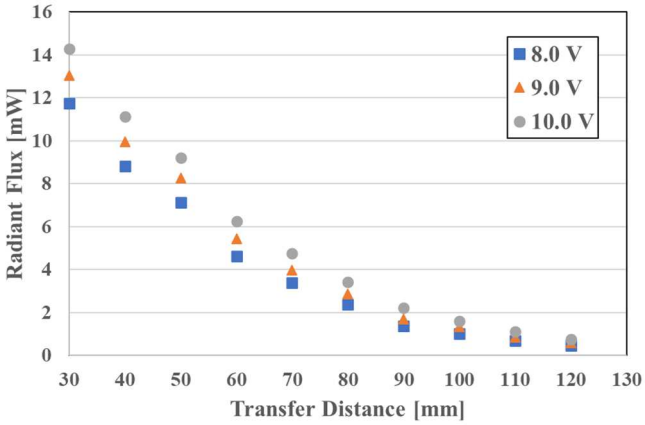

Fig. 7 Measurement of the variation of the radiant flux from the LEDs at different input voltages(8-10 V) with different transfer distances(30-120 mm).

B. Distribution Evaluation of Radiant Flux from LEDs

We evaluated whether sufficient photoirradiation was provided to the cell surface to be cultured when conducting cell experiments with the WPT device. The well plates in which cancer cells are cultured in cell experiments is shown in Fig. 8. The standard for this well plate is cylindrical with a depth of 15 mm and a diameter of 22 mm.

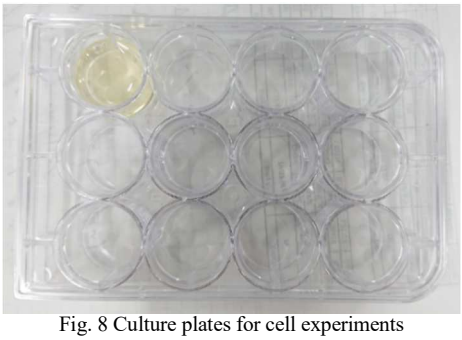

Fig. 8 Culture plates for cell experiments

In the above wells, the distribution of the radiant flux from the LEDs at the cancer cell surface to be cultured was evaluated using a schematic diagram (Fig. 9). The directional angle of this LED is 120 degrees. Fig. 9 simulates the arrangement of the six LEDs on the receiving device. Fig. 9 shows that more than 80 % of the radiant flux from the LEDs can be maintained even at the edge of the cell surface to be cultured, which is the furthest from the LEDs.

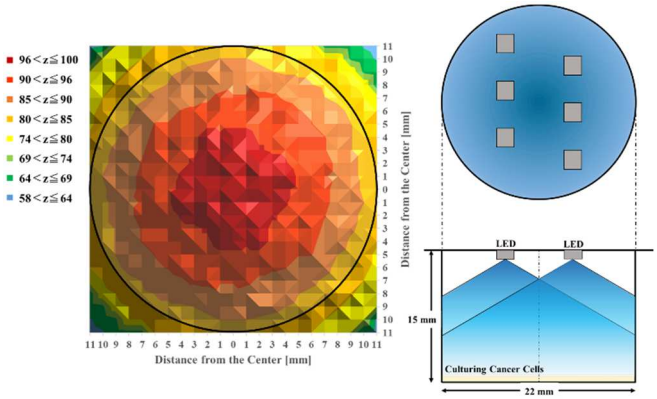

Fig. 9 Distribution evaluation of radiant flux from LEDs

C. Generation of Singlet Oxygen

The generation of singlet oxygen, which has toxicity to cancer cells, was evaluated by photoirradiation using the experimental equipment (Fig. 10). The decomposition of Diphenylisobenzofuran (DPBF) by singlet oxygen was tracked using a blue light LED with a wavelength of 470 nm and a cyclometalated iridium(Ir(III)) complexes [22], a photosensitizer that reacts to blue light. The protocol for the generation of singlet oxygen is shown in Fig. 11.

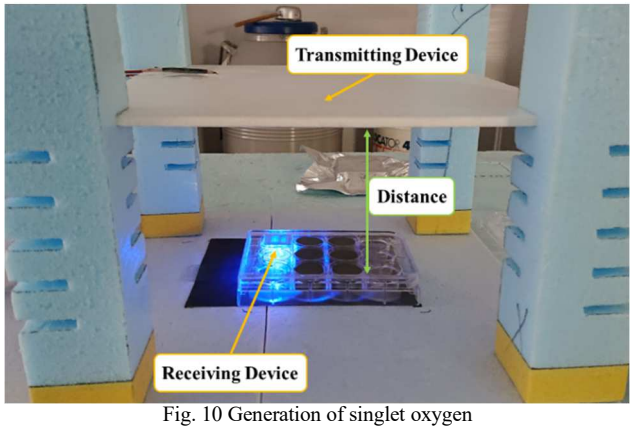

Fig. 10 Generation of singlet oxygen

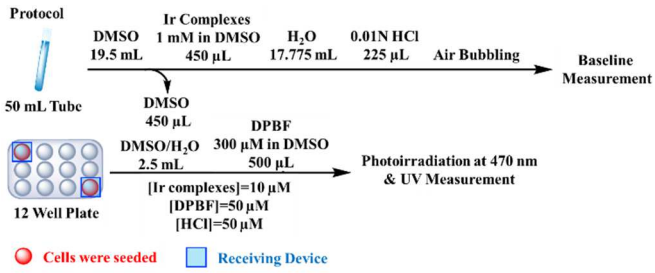

Fig. 11 The protocol for the generation of singlet oxygen

The variation of the absorbance spectrum of DPBF in Fig. 12 indicates that DPBF has a specific maximum absorbance at 415 nm. Each spectrum represents a photoirradiation time of 0, 2, 4, 6, 8, and 10 minutes in order from the top. The decrease of absorbance with photoirradiation over time suggested that the singlet oxygen generated by photoirradiation with WPT

decomposes DPBF. When the transfer distance was fixed at 120 mm, the percentage remaining amount of DPBF was 32 % and 7 % after 10 minutes of photoirradiation at 8 V and 10 V input voltages, respectively, as shown in Fig. 13. Therefore, it indicated that the amount of singlet oxygen generated increased in dependence on the input voltage. Also, the percentage remaining amount of DPBF is almost unvaried since the decomposition of DPBF proceeds slowly in the absence of the Ir(III) complexes.

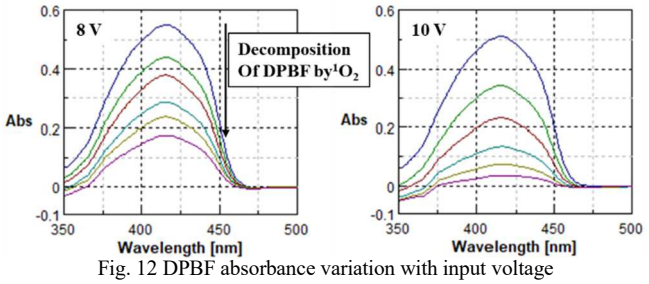

Fig. 12 DPBF absorbance variation with input voltage

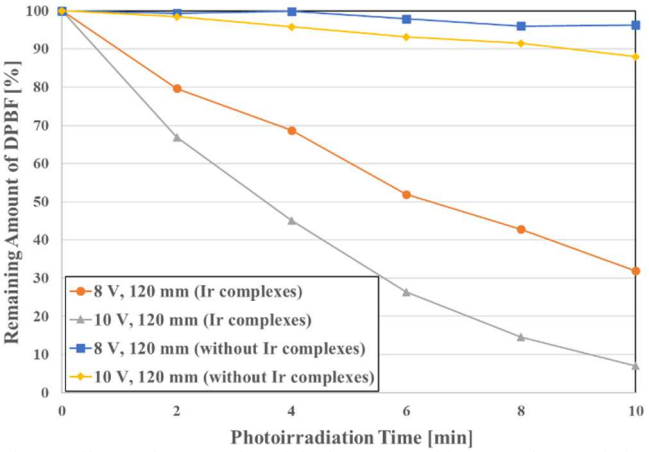

Fig. 13 Effect on the generation of singlet oxygen with input voltage variation

The same experiment was conducted with the input voltage fixed at 8 V and the transfer distance varied. As a result, Figs. 14 and Fig. 15 indicate that the percentage remaining amount of DPBF was 6 % and 32 % after 10 minutes of photoirradiation at transfer distances of 100 mm and 120 mm, respectively. Therefore, it was also indicated that the amount of singlet oxygen generated increased depending not only on the photoirradiation time but also on the transfer distance.

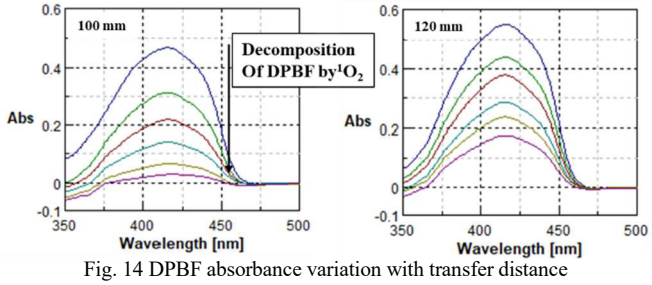

Fig. 14 DPBF absorbance variation with transfer distance

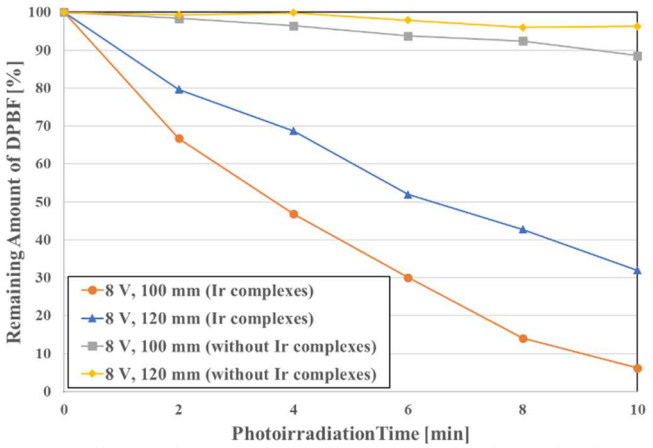

Fig. 15 Effect on the generation of singlet oxygen with transfer distance variation

V. Inducing Cancer Cell Death

Inducing cancer cell death was performed using the WPT system shown in Fig. 16. Cancer cell death induced by singlet oxygen generated by photoirradiation of WPT using human uterine cervical cancer cells (HeLa-S3) and Ir(III) complexes, was evaluated using nucleic acid staining dye (Propidium iodide: PI). PI does not permeate the cell membrane of living cells, but migrates into the nucleus of dead cells and emits a remarkable red fluorescence as it is incorporated into the DNA. The protocol for inducing cancer cell death is shown in Fig. 17.

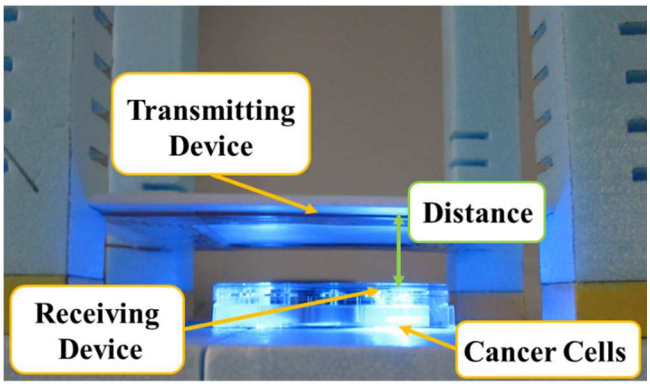

Fig. 16 Inducing cancer cell death

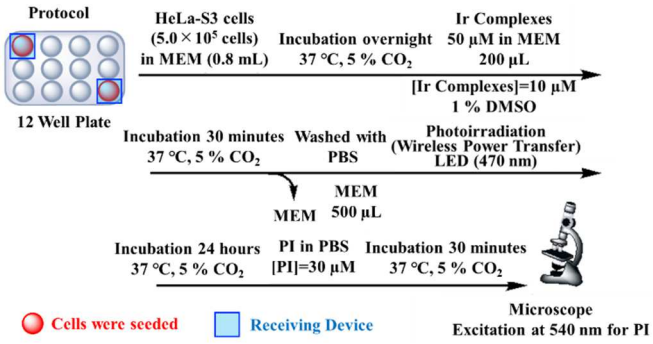

Fig. 17 The protocol for inducing cancer cell death

Fluorescence microscopy images of HeLa-S3 cells are shown in Fig. 18 under the reaction conditions in Table 2 with an input voltage of 10 V, a transfer distance of 30 mm, and an incubation time of 24 hours after photoirradiation. The photoirradiation times were 30, 40, 50, and 60 minutes. In Entry 1, Entry 3, Entry 5, and Entry 7, where Ir(III) complexes were absent, there was little or no induction of cancer cell death by photoirradiation. On the other hand, in Entry 2, Entry

4, Entry 6, and Entry 8, where Ir(III) complexes were present, the cancer cells were remarkably stained red and fluorescent. These results indicate that cancer cell death was induced by singlet oxygen generated by photoirradiation.

Table 2 Reaction conditions

Entry	Photosensitizer	Transfer Distance [mm]	Photoirradiation Time [min]
1	—	30	30
2	Ir(III) complexes	30	30
3	—	30	40
4	Ir(III) complexes	30	40
5	—	30	50
6	Ir(III) complexes	30	50
7	—	30	60
8	Ir(III) complexes	30	60

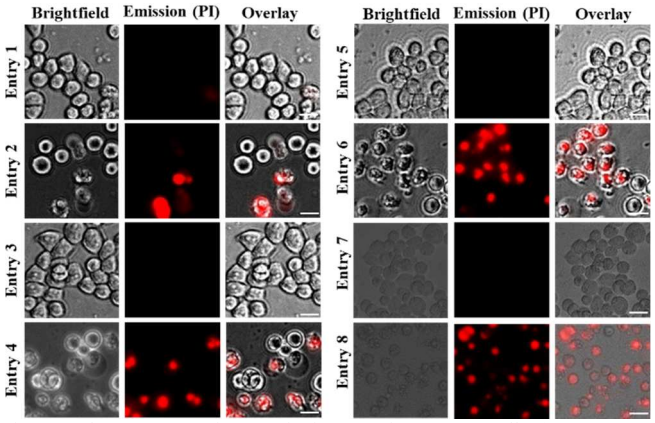

Fig. 18 Fluorescence microscopic image of HeLa-S3 cells (Entry 1: 30 minutes photoirradiation, without Ir(III) complexes), (Entry 2: 30 minutes photoirradiation, Ir(III) complexes), (Entry 3: 40 minutes photoirradiation, without Ir(III) complexes), (Entry 4: 40 minutes photoirradiation, Ir(III) complexes), (Entry 5: 50 minutes photoirradiation, without Ir(III) complexes), (Entry 6: 50 minutes photoirradiation, Ir(III) complexes), (Entry 7: 60 minutes photoirradiation, without Ir(III) complexes), (Entry 8: 60 minutes photoirradiation, Ir(III) complexes). The white scale bar is 20 µm.

Next, we investigated the effects of photoirradiation time on cancer cell death. As shown in Fig. 19, the number of cancer cells stained red increased as the photoirradiation time increased to 30, 40, 50, and 60 minutes, which means that the percentage of inducing cell death increased to 4, 35, 65, and 75 %.

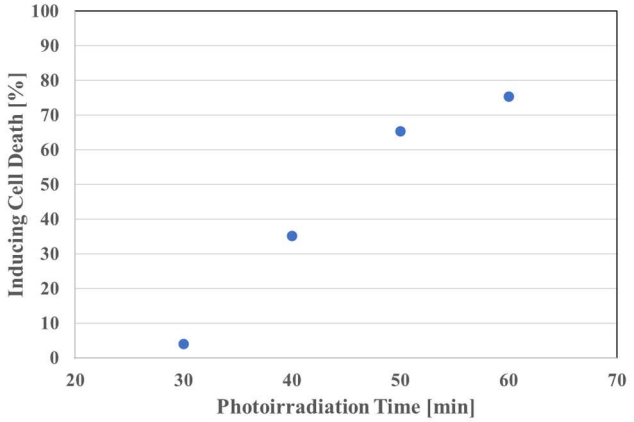

Fig. 19 Percentage of inducing cancer cell death

VI. Amount of Light Energy and Percentage of Inducing Cell Death

Based on the percentage of inducing cell death described in the previous chapter, we evaluated the relationship between the amount of light energy irradiated to cancer cells and the percentage of inducing cell death. Using equation (1), which is a relation for the cumulative amount of light energy, we derived the relationship between the amount of light energy irradiated in the experiment described in the previous chapter and the percentage of cell death, and also derived an approximation of the amount of light energy required to induce 100 % cell death. The results are shown in Table 3. The radiant flux with wired in Table 3 (66.3 mW) was measured using the photoirradiation device [22]. Based on Table 3, Fig. 20 shows the amount of light energy irradiated and the percentage of cell death, and Fig. 21 shows the approximation of the amount of light energy required to induce cell death at 100 % with wired and wireless photoirradiation.

$$J = W \cdot s \tag{1}$$

In equation (1), J is the cumulative amount of light energy [J], W is the radiant flux from the LED [W], and s is the photoirradiation time [s].

As shown in Fig. 20, the percentage of inducing cancer cell death increased with increasing the amount of light energy irradiated. A strong positive correlation coefficient of 0.91 was also indicated. As shown in Fig. 21, it was suggested that about 60-100 J or 100-140 J/cm^2 of light energy irradiated was required as an approximation to induce 100 % cancer cell death. In this case, conditions with a percentage of cell death less than 10 % in Table 3 were excluded because the cancer cell proliferation was considered to be significant.

Table 3 Amount of light energy and percentage of inducing cell death

Radiant Flux [mW]	Photoirradiation Time [min]	Inducing Cell Death [%]	The Amount of Light Energy [J]	Energy Required for Inducing 100 % Cell Death [J]
66.3	20	95	79.56	83.75
14.28	30	4.1	25.70	627.0
14.28	40	35.2	34.27	97.36
14.28	50	65.3	42.84	65.60
14.28	60	75.4	51.41	68.18

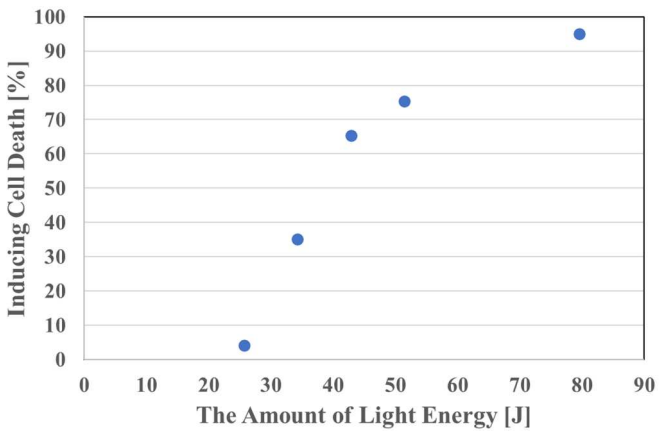

Fig. 20 Amount of light energy and percentage of inducing cell death

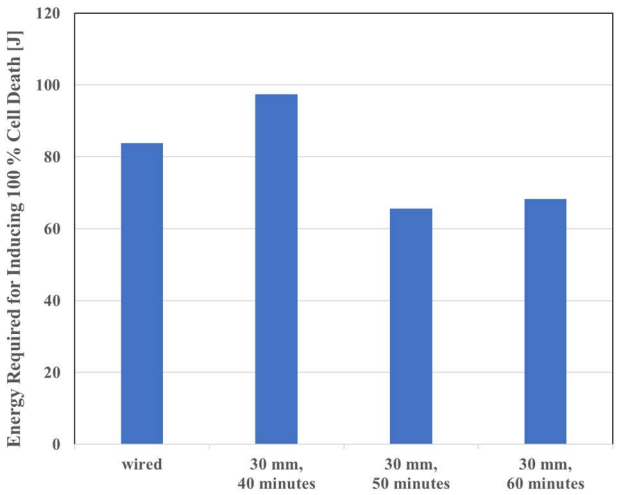

Fig. 21 Amount of light energy required for inducing 100 % cell death

VII. Conclusion

In this paper, we proposed methods of cancer treatment that integrate WPT and PDT with 6.78 MHz as the operating frequency and verified its significance by circuit simulations and experiments. A WPT system that combined a small and lightweight receiving coil and LEDs for implantation in the body was designed based on circuit simulations, and evaluated in terms of engineering and pharmaceuticals. After engineering evaluation based on two characteristics of LEDs, current value and radiant flux, and pharmaceutical evaluation based on singlet oxygen generation by drug reaction experiments using DPBF, this WPT system was confirmed in advance to have sufficient performance for inducing cancer cell death. After that, cancer cell death was induced in vitro as a basic experiment for cancer treatment. Under the condition of 30 mm transfer distance in free space, about 75 % of cancer cell death was induced successfully by 60 minutes of photoirradiation. These results demonstrated the expanded possibilities for cancer treatment by integrating WPT and PDT.

Also, in this paper, the approximation of the amount of light energy required when using the Ir(III) complexes and the method is derived based on the percentage of inducing cancer cell death. Based on the results, it was indicated that about 60-100 J or 100-140 J/cm^2 of light energy irradiation is required, which enabled the prediction of the required photoirradiation time, or treatment time depending on the radiant flux from the light source.

Future study includes optimization of the WPT system. Thus, enhancement of the treatment outcome can be expected by enabling highly efficient transmission to small receiving devices. In addition, the study of power transfer through biological tissues, and the investigation of the effects of such power transfer and how to deal with them are also included.

References

[1] A. Kurs, A. Karalis, R. Moffatt, J. D. Joannopoulos, P. Fisher, and M. Soljačić, "Wireless Power Transfer via Strongly Coupled Magnetic Resonances," *Science*, vol. 317, no. 5834, pp. 83–86, July 2007.

[2] S. Li and C. C. Mi, "Wireless Power Transfer for Electric Vehicle Applications," in *IEEE Journal of Emerging and Selected Topics in Power Electronics*, vol. 3, no. 1, pp. 4-17, March 2015.

[3] R. Tavakoli and Z. Pantic, "Analysis, Design, and Demonstration of a 25-kW Dynamic Wireless Charging System for Roadway Electric Vehicles," in *IEEE Journal of Emerging and Selected Topics in Power Electronics*, vol. 6, no. 3, pp. 1378-1393, Sept. 2018.

[4] K. Sasaki and T. Imura, "Combination of Sensorless Energized Section Switching System and Double-LCC for DWPT," *2020 IEEE PELS Workshop on Emerging Technologies: Wireless Power Transfer (WoW)*, pp. 62-67, Nov. 2020.

[5] S. Nguyen, C. Duong and R. Amirtharajah, "A Smart Health Tracking Ring Powered by Wireless Power Transfer," *2021 IEEE Wireless Power Transfer Conference (WPTC)*, pp. 1-4, 2021.

[6] S. -M. Kim, I. -K. Cho, S. -W. Kim, J. -I. Moon and H. -J. Lee, "A Qi-compatible Wireless Charging Pocket for Smartphone," *2020 IEEE Wireless Power Transfer Conference (WPTC)*, pp. 387-390, 2020.

[7] Y. Liu, Y. Li, J. Zhang, S. Dong, C. Cui and C. Zhu, "Design a Wireless Power Transfer System with Variable Gap Applied to Left Ventricular Assist Devices," *2018 IEEE PELS Workshop on Emerging Technologies: Wireless Power Transfer (Wow)*, pp. 1-5, 2018.

[8] T. Campi, S. Cruciani, F. Maradei, A. Montalto, F. Musumeci and M. Feliziani, "Centralized High Power Supply System for Implanted Medical Devices Using Wireless Power Transfer Technology," *in IEEE Transactions on Medical Robotics and Bionics*, vol. 3, no. 4, pp. 992-1001, Nov. 2021.

[9] S. Hong et al., "Cochlear Implant Wireless Power Transfer System Design for High Efficiency and Link Gain Stability using A Proposed Stagger Tuning Method," *2020 IEEE Wireless Power Transfer Conference (WPTC)*, pp. 26-29, 2020.

[10] D. Mukherjee and D. Mallick, "Experimental Demonstration of Miniaturized Magnetoelectric Wireless Power Transfer System For Implantable Medical Devices," *2022 IEEE 35th International Conference on Micro Electro Mechanical Systems Conference (MEMS)*, pp. 636-639, 2022.

[11] S. G. Jang, J. Kim, J. Lee, J. S. Kim, D. Hwan Kim and S. M. Park, "Wireless Power Transfer Based Implantable Neurostimulator," *2020 IEEE Wireless Power Transfer Conference (WPTC)*, pp. 365-368, 2020.

[12] Y. Ma, Z. Luo, C. Steiger, G. Traverso, and F. Adib, "Enabling Deep-Tissue Networking for Miniature Medical Devices," *Proc. ACM SIGCOMM 2018 Conference*, pp. 417-431, Aug. 2018.

[13] Mitsunaga M, Nakajima T, Sano K, Choyke PL, Kobayashi H, "Near-infrared Theranostic Photoimmunotherapy (PIT): Repeated Exposure of Light Enhances the Effect of Immunoconjugate," *Bioconjugate Chemistry* 2012, 23(3), 604-409.

[14] P. M. Lee, X. Tian and J. S. Ho, "Wireless Power Transfer for Glioblastoma Photodynamic Therapy," *2019 IEEE Biomedical Circuits and Systems Conference (BioCAS)*, pp. 1-4, 2019.

[15] Kirino, I., Fujita, K., Sakanoue, K. et al., "Metronomic photodynamic therapy using an implantable LED device and orally administered 5-aminolevulinic acid," *Scientific Reports 10*, Dec. 2020.

[16] Kim, A., Zhou, J., Samaddar, S. et al., "An Implantable Ultrasonically-Powered Micro-Light-Source (μLight) for Photodynamic Therapy", *Scientific Reports 9*, Feb. 2019.

[17] Y. Yoshitaka, T. Imura, Y. Hori, K. Yokoi, A. Kanbe, M. Kakihana and S. Aoki, "A basic experiment with cancer cells for photodynamic therapy by wireless power transfer," *IEICE Technical Report*, vol. 121, no. 289, WPT2021-14, pp. 5-8, Dec. 2021.

[18] B. Strassner and K. Chang, "Microwave Power Transmission: Historical Milestones and System Components," in *Proceedings of the IEEE*, vol. 101, no. 6, pp. 1379-1396, June 2013.

[19] M. Meng and M. Kiani, "Design and Optimization of Ultrasonic Wireless Power Transmission Links for Millimeter-Sized Biomedical Implants," in *IEEE Transactions on Biomedical Circuits and Systems*, vol. 11, no. 1, pp. 98-107, Feb. 2017.

[20] T. Imura and Y. Hori, "Maximizing Air Gap and Efficiency of Magnetic Resonant Coupling for Wireless Power Transfer Using Equivalent Circuit and Neumann Formula," in IEEE Transactions on Industrial Electronics, vol. 58, no. 10, pp. 4746-4752, Oct. 2011.

[21] M. P. Theodoridis, "Effective Capacitive Power Transfer," in *IEEE Transactions on Power Electronics*, vol. 27, no. 12, pp. 4906-4913, Dec. 2012.

[22] A. Kando, Y. Hisamatsu, H. Ohwada, T. Itoh, S. Moromizato, M. Kohno, and S. Aoki, "Photochemical Properties of Red-Emitting Tris(cyclometalated) Iridium(III) Complexes Having Basic and Nitro Groups and Application to pH Sensing and Photoinduced Cell Death," *Inorg Chem. 2015*, vol. 54, no. 11, pp. 5342-5357, Jun 2015.